Heliyon 9 (2023) e16755

Contents lists available at ScienceDirect

Heliyon

journal homepage: www.cell.com/heliyon

Electroacupuncture at ST 36 ameliorates cognitive impairment and beta-amyloid pathology by inhibiting NLRP3 inflammasome activation in an Alzheimer's disease animal model

Hong Ni [c,1], Jiaoqi Ren [e,1], Qimeng Wang [f], Xing Li [c], Yue Wu [c], Dezhi Liu [d,**], Jie Wang [a,b,c,*]

[a] Endocrinology department of Shanghai Municipal Hospital of Traditional Chinese Medicine, Shanghai University of Traditional Chinese Medicine, Shanghai, 200071, China
[b] Department of Peripheral Vascular Surgery, Shuguang Hospital Affiliated to Shanghai University of Traditional Chinese Medicine, 201203, Shanghai, China
[c] Academy of Integrative Medicine, Shanghai University of Traditional Chinese Medicine, 201203, Shanghai, China
[d] Department of Neurology, Shuguang Hospital Affiliated to Shanghai University of Traditional Chinese Medicine, 201203, Shanghai, China
[e] Department of Geriatrics, Huashan Hospital, National Clinical Research Center for Aging and Medicine, Fudan University, 200040, Shanghai, China
[f] Department of Acupuncture, Yueyang Hospital of Integrated Traditional Chinese and Western Medicine, Shanghai University of Traditional Chinese Medicine, Shanghai, 200437, China

ARTICLE INFO

Keywords:
Alzheimer's disease
5×FAD mice
Electroacupuncture
ST 36
NLRP3 inflammasome

ABSTRACT

Background: Alzheimer's disease (AD) is the most prevalent neurodegenerative disorder leading to cognitive impairment in the elderly, and no effective treatment exists. Increasing evidence has demonstrated that physical therapy and electroacupuncture (EA) effectively improve spatial learning and memory abilities. Nevertheless, the mechanism underlying the effects of EA on AD pathology is largely unexplored. Acupuncture at Zusanli (ST 36) has previously been shown to improve cognitive impairment in AD, but the mechanism is unclear. According to recent studies, EA drives the vagal–adrenal axis from the hindlimb ST 36 acupoint but not from the abdominal Tianshu (ST 25) to curb severe inflammation in mice. This study examined whether ST 36 acupuncture improves cognitive dysfunction in AD model mice by improving neuroinflammation and its underlying mechanism.

Methods: Male 5xFAD mice (aged 3, 6, and 9 months) were used as the AD animal model and were randomly divided into three groups: the AD model group (AD group), the electroacupuncture at ST 36 acupoint group (EA-ST 36 group), and the electroacupuncture at ST 25 acupoint group (EA-ST 25 group). Age-matched wild-type mice were used as the normal control (WT) group. EA (10 Hz, 0.5 mA) was applied to the acupoints on both sides for 15 min, 5 times per week for 4 weeks. Motor ability and cognitive ability were assessed by the open field test, the novel object recognition task, and the Morris water maze test. Thioflavin S staining and immunofluorescence were

* Corresponding author. Endocrinology Department of Shanghai Municipal Hospital of Traditional Chinese Medicine, Shanghai University of Traditional Chinese Medicine, Shanghai, 200071, China.
** Corresponding author. Department of Neurology, Shuguang Hospital Affiliated to Shanghai University of Traditional Chinese Medicine, 201203, Shanghai, China
E-mail addresses: sgliudezhi@shutcm.edu.cn (D. Liu), wangjieyct@163.com (J. Wang).
[1] Hong Ni and Jiaoqi Ren have contributed equally to this article.

https://doi.org/10.1016/j.heliyon.2023.e16755
Received 15 August 2022; Received in revised form 9 April 2023; Accepted 25 May 2023
Available online 27 May 2023
2405-8440/© 2023 The Authors. Published by Elsevier Ltd. This is an open access article under the CC BY-NC-ND license (http://creativecommons.org/licenses/by-nc-nd/4.0/).

used to mark Aβ plaques and microglia. The levels of NLRP3, caspase-1, ASC, interleukin (IL)-1β, and IL-18 in the hippocampus were assayed by Western blotting or qRT-PCR.
Results: EA at ST 36, but not ST 25, significantly improved motor function and cognitive ability and reduced both Aβ deposition and microglia and NLRP3 inflammasome activation in 5×FAD mice.
Conclusion: EA stimulation at ST 36 effectively improved memory impairment in 5×FAD mice by a mechanism that regulated microglia activation and alleviated neuroinflammation by inhibiting the NLRP3 inflammatory response in the hippocampus. This study shows that ST 36 may be a specific acupoint to improve the condition of AD patients.

1. Introduction

Alzheimer's disease (AD) is the most prevalent neurodegenerative disorder leading to progressive cognitive impairment in the elderly, beginning with memory deterioration and followed by dysfunction and psychiatric problems [1]. The brains of AD patients are characterized by an accumulation of extracellular beta-amyloid (Aβ) plaques and the deposition of intracellular neurofibrillary tangles (NFTs) [2]. Although the pathology of AD has been characterized, the mechanisms of neuronal loss and cognitive impairment in AD remain elusive [3,4]. Most therapeutic agents used to clinically treat AD target Aβ and NFTs but do not stop or reverse disease progression. More attention has been given to the critical role of neuroinflammation in the pathogenesis of AD. Neuroinflammation is involved in every aspect of AD pathology and has been termed the third core pathology of AD [5–7].

As the major component of the innate immune system in the brain, microglia play an important role in inflammation, particularly the amyloid plaque burden [1]. Chronically activated microglia become dysfunctional and release excess pro-inflammatory cytokines and chemokines, including cyclooxygenase-2, interleukin (IL)-1β, IL-6, and tumor necrosis factor (TNF)-α, followed by an inflammatory cascade, which may result in an increased level of hyperphosphorylated tau, Aβ accumulation, and gliosis [8]. Activation of the pyrin-domain-containing protein 3 (NLRP3) inflammasome from the NOD-like receptor (NLR) family, which contributes to the expression of IL-1β in the brain, is fundamental to subsequent inflammatory events [9]. Therefore, inhibiting or depleting the NLRP3 inflammasome represents a new therapeutic interventional strategy for AD [10].

Electroacupuncture (EA) is a traditional Chinese medical treatment that has been used to activate neuronal networks and modulate the functions of the brain to treat various neurodegenerative diseases, including AD [11,12], Parkinson's disease [13], and vascular dementia [14]. Many studies have suggested that EA improves spatial learning memory, promotes the degradation of Aβ [15], and alleviates the neuroinflammatory reaction in the hippocampus [16] in the AD mouse model [17]. Acupuncture at Zusanli (ST 36) has previously been shown to improve cognitive impairment in AD, but the mechanism is unclear [18]. ST 36 is located 2 cm below the knee in humans and is the most effective stimulation to relieve inflammation [19]. ST 36 drives the vagal–adrenal anti-inflammatory axis in mice by stimulating neurons that highly express PROKR2 [20,21], and stimulating ST 36 activates PROKR2-expressing peripheral sensory fibers located in the dorsal root ganglion so that sensory information is transmitted to the nucleus tractus solitaire, which, in turn, activates the vagus nerve and promotes the release of catecholamines from the adrenal gland, thereby inhibiting inflammation [22]. Unfortunately, it is unknown whether acupuncture at ST 36 reduces neuroinflammation in the brain and improves cognitive dysfunction by regulating NLRP3 inflammasome signaling. Furthermore, sensory fibers expressing PROKR2 are more concentrated in the limbs than in the abdomen, which explains the poor anti-inflammatory effect of stimulating ST 25 [22,23]. Thus, ST 25 is often used as a negative control for ST 36.

Therefore, to explore the possible mechanisms underlying cognitive improvement after acupuncture of ST 36 in 5×FAD transgenic mice, a mouse AD model with a quickly developing AD pathology was used. This model presents with Aβ accumulation and neuroinflammation at 2 months of age and cognitive dysfunction at 5 months of age [24]. A combination of behavioral experiments was conducted to investigate the motor and cognitive functions of AD mice during different months. Additionally, molecular biology experiments were performed to investigate the internal mechanisms. The purpose of this study was to provide a theoretical basis for clinically applying acupuncture at ST 36 to treat AD.

2. Materials and Methods

2.1. Animal grouping

The 5xFAD male mice as well as the C57BL/6 mice of the same age were obtained from Nanjing University's Model Animal Research Center and bred at Shanghai University of Traditional Chinese Medicine's Experimental Animal Center. Male 5xFAD mice and C57BL/6 mice aged 3, 6 and 9 months were used in studies. Under a 12-h light/dark cycle (Light on 07:00 a.m.–19:00 p.m.) and with access to sterile drinking water and standard food, the animals were housed in a facility with a temperature of 22 °C and humidity of 55 °C. 3-m, 6-m, 9-m male 5xFAD and age-matched C57BL/6 were randomly divided into the following four groups respectively using a random number table: 5xFAD, 5xFAD + ST36, 5xFAD + ST25 and WT-Con. Thirty 3-month-old male 5xFAD transgenic mice were assigned randomly and equally into three groups, control group (5xFAD), EA at ST36 group (EA-ST36) and EA at ST25 group (EA-ST25). Another ten 3-m C57BL/6 mice were used as normal group (WT group). The thirty male 6-month-old and thirty male 9-month-old 5xFAD mice were grouped in the same way with ten male age-matched WT mice each group. The mice were acclimated for 7 days

before the experiment. After the EA, half of the mice in each group were intraperitoneally anesthetized with 10% chloral hydrate immediately after the behavioral tests and intraperitoneally perfused with 4% paraformaldehyde (PFA) for brain tissue sections. The remaining mice were sacrificed by rapid decapitation for Western blot analysis and qRT-PCR. All experimental protocols were in strict accordance with the regulations of the National Institutes of Health guide for the care and use of laboratory animals, formulated by the Ministry of Science and Technology of the People's Republic of China and were approved by the Animals Research Ethics Committee of Shanghai University of Chinese Medicine (No. PZSHUTCM200821019).

2.2. Electroacupuncture

EA treatment was conducted based on the previous research [22]. EA treatment was administered to 5xFAD mice at ST25 or ST36. We anesthetized mice with isoflurane (0.5–1.5%) (Sigma, USA), then placed them on a heating pad (Sider Technology, China) to maintain their body temperatures. 75% alcohol was used to clean the skin around the acupoints before stainless steel needles (diameter 0.17 mm, length 7 mm) were inserted in ST36 or ST25 at a depth of 4 mm. ST36 acupoints situate about 4 mm lower from the knee joint and approximately 2 mm lateral to the anterior tubercle of the tibia. ST25 acupoints situate at the intersections defined by 5 mm lateral to, and the upper two-thirds and the lower one-third of, the line between the xiphoid process and the pubic symphysis upper border (Fig. 1A). Needle handles were connected to a acupuncture apparatus (Wuxi Jiajian Medical Instrument Co.,Ltd., China) and EA treatment was conducted for 15 min (0.5 mA, 10 Hz). For four weeks, it was performed five times per week.

2.3. Morris water maze (MWM)

To evaluate the cognitive abilities of mice, a MWN test was used [25]. The mice were allowed to swim in a round pool (120 cm in diameter and 40 cm in height), which was full of opaque water (20–22 °C) with non-toxic white paint. Special markers were attached to the fixed position around the pool. A platform (diameter 8 cm) was hidden 1 cm below the surface of the water. There was a video tracking system installed over the pool to monitor mouse swimming trajectory and record escape latency. Mice were trained to locate the hidden platform by following clues surrounding the pool in 60 s. After 60 s, if the mouse has not found the platform, it should be guided there and asked to remain there for 20 s. The trail was conducted immediately after 4 weeks EA treatment, each mouse was tested for 3 trials and starting point of each trail was in different quarters in the afternoon for 6 days to find the platform below the water surface. The whole procedures were recorded by the ZS-001 system (Beijing, China). On the last day, the latency to reach the platform place, the crossing times to the platform regions, the percent time with in the target quadrant, as well as the swimming velocity was recorded after the platform was removed.

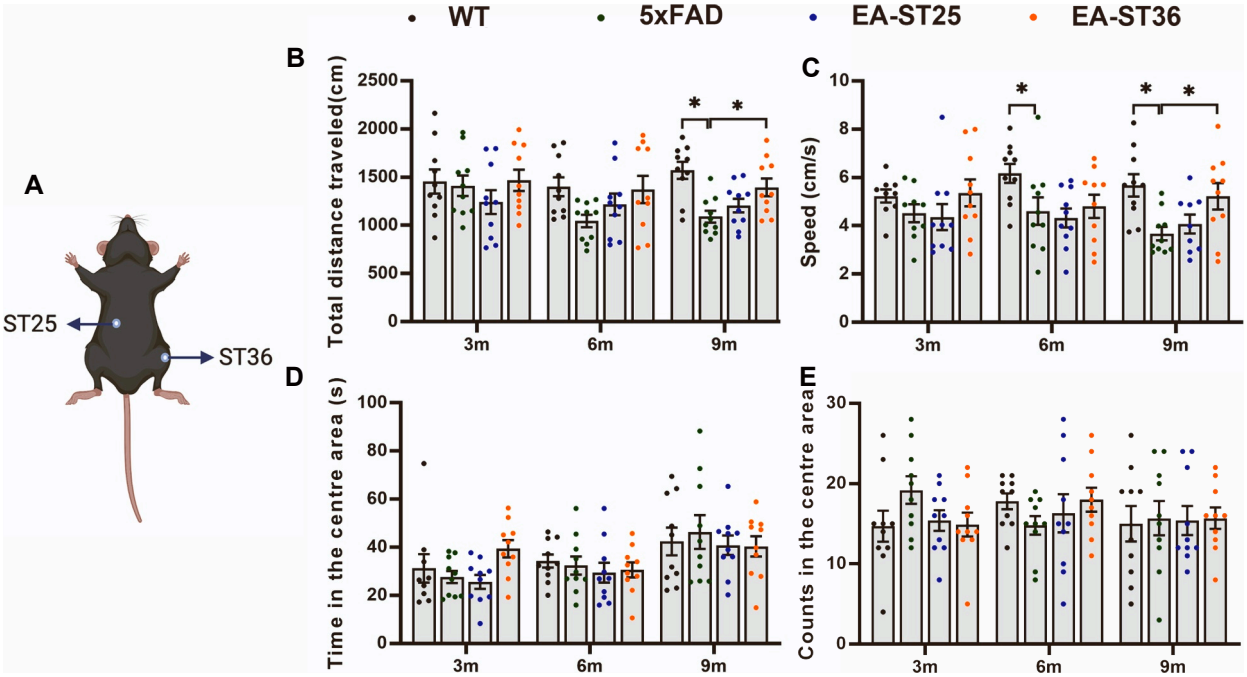

Fig. 1. Effect of EA on the motor function of 5×FAD mice detected by OFT. **(A)** The location of ST36 and ST25. **(B)** Total distance traveled within 5 min. **(C)** Average speed. **(D)** Time stayed in the center area. **(E)** Counts crossing the center area. (The bars indicate the means ± SEM; n = 10 per group; *$p < 0.05$).

2.4. Open field test (OFT)

It was designed to assess motor ability as well as behavior indicative of anxiety. This test was conducted immediately after 4 weeks EA treatment. During a 5-min period, mice were permitted to move spontaneously in the square area with white walls and floor (50 × 50 × 40 cm). With the aid of a tracking system installed above the open field, speed and distance traveled by the mice, as well as the duration spent in the center region, were monitored and analyzed. A 75% ethanol solution was used to clean the floor and walls between each session.

2.5. The novel object recognition task (NORT)

During NORT, all the mice were permitted to discover novel versus familiar objects in order to evaluate their memory performance of recognizing novel objects versus familiar objects [26]. On the day one after MWM, all the mice were allowed to accustom to an open-field arena (50 cm × 50 cm, dim light, 24 °C) and two blocks in it for 10 min twice a day for two consecutive days. On the third day, each mouse was allowed to explore blocks for 5 min, and then 5 min in cage, after which mouse was placed back to arena, in which one block was replaced by a novel plastic cylinder, and subjected to short-term memory test (STM). For long-term memory (LTM), the interval was 24 h and the familiar or novel objects were replaced. A discrimination index (DI) was used to assess memory. Basically, the DI is calculated by comparing the time spent exploring a novel object with the whole amount of time spent on both.

2.6. Thiofavin S staining

After soaked in a 30% sucrose solution for 2 days, the brain tissue was sliced at 10 μm with the cryostat microtome (Leica). A 0.3% potassium permanganate solution was applied for 5 min, 1% oxalic acid was applied for 5 min, and a 1% sodium borohydride solution was applied for 5 min, followed by two PBS washes. After washing in PBS, glass coverslips was used for mounting the brain sections and dried, followed by 1% thioflavin S (Sigma, USA) diluted in 50% ethanol solution staining for 8 min in the dark. After dehydrating the sections in 80%, 90% and 100% ethanol for 5 min, the sections were mounted using fluorescent mounting medium (Sigma, USA). Sections were observed and photographed using a fluorescence microscope (Zeiss, Thornwood, NY, USA). We analyzed the amount of Aβ plaques in the hippocampus and cortex regions as previously mentioned [27].

2.7. Immunofluorescence

The brain sections were blocked for 10 min with 3% BSA in PBS and then incubated for one night at 4 °C by the primary antibodies Iba-1 (Rabbit monoclonal) (1:500; Abcam, USA). Subsequently, the sections were incubated with the secondary antibodies [1:1000 Alexa Fluor 555-conjugated anti-rabbit (Thermo Fisher Scientific, USA)] for 2 h. Three times 10 min rinses in PBS were conducted following each of the aforementioned steps. In the final step, fluorescent mounting medium (Sigma, USA) was applied to the sections. Laser-scanning confocal microscopes (Leica TCS SP2, Germany) were used to capture confocal images. Microglia were analyzed based on their branching lengths and number of branching endpoints as determined in the previous study [28].

2.8. Western blot

Assay buffer containing a protease and phosphatase inhibitor mixture was used to isolate the protein from hippocampus by radioimmunoprecipitation (RIPA). It is recommended to homogenize, sonicate and centrifuge the brain cells at 14,000 g and 4 °C for 15 min as soon as they have been suspended. A BCA Protein Assay kit (Thermo Fisher Scientific, USA) was used to determine the protein concentration. Following this, the proteins were boiled at 100 °C for 10 min in a buffer that contained glycerol, Eagle's medium, and SDS. Proteins were separated using SDS-PAGE at 12.5% (Yeasen Biotech, China), and then transferred to nitrocellulose membranes (Yeasen Biotech, China). Then the membranes should be blocked by 5% BSA within the TBST buffer (10 mmol/L of Tris, pH 7.5; 100 mmol/L of NaCl; and 0.1% Tween 20), and was incubated overnight at 4 °C with specific primary antibodies (1:1000) of NLRP3 (Cell Signaling, USA), Caspase-1 (Cell Signaling, USA), ASC (Cell Signaling, USA), IL-1β (Cell Signaling, USA), Beta Tubulin (Proteintech, USA). On the second day, the primary antibody was detected with anti-rabbit (or anti-goat/mouse) secondary antibodies (1:5000; Invitrogen, USA) and the immunoreactive bands were visualized with an enhanced chemiluminescence kit (Beyotime Biotechnology, China), then at the end Image J software was used to evaluate band density. A minimum of three blots were performed for each condition.

2.9. RNA extraction and real-time PCR

A total RNA extract from mouse hippocampus was extracted using 800 ml Trizol (Invitrogen, USA) in order to determine the expression of mRNA. As part of the measurement, NanoDrop 2000 micro-ultraviolet spectrophotometry (1011U, NanoDrop Technologies, USA) was used to determine the purity and concentration of RNA. The reverse transcription of RNA into cDNA was performed based on the manuscript provided by the cDNA Reverse Transcription Kit (Takara Bio Inc, Japan). Quantitative real-time PCR was performed with SYBR Premix Ex Taq II (Takara, Japan) using an ABI StepOnePlus Real-Time PCR System (Thermo Fisher Scientific, USA), and the primers were synthetized by the Takara Biotechnology Co., Ltd. (Japan). We conducted the PCR procedure as follows: 95 °C for 30 s, followed by 40 cycles of 95 °C for 5 s, followed by 60 °C for 34 s. The expression levels of target genes were calculated by

normalizing the cycle threshold (Ct) values to the glyceraldehyde-3-phosphate dehydrogenase (GAPDH), and calculated based on the $2^{-\Delta\Delta Ct}$ method [29]. The primer sequences are: IL-1β, forward: ATCTCGCAGCAGCACATCAAC, reverse: TGTTCATCTCGGAGCCTGTAGT; IL-18, forward: CAGGCCTGACATCTTCTGCAA, reverse: TCTGACATGGCAGCCATTGT; NLRP3, forward: GACACGAGTCCTGGTGACTTT, reverse: GATGATGTTGGCAGCAATGG; GAPDH, forward: GCCAAATTCAACGGCACAGT, reverse: AGATGGTGATGGGCTTCCC.

2.10. Statistical analysis

Apart data from the behavioral experiment were presented as means ± SEM. Statistical analyses were tested by GraphPad Prism (GraphPad9.0, USA). One-way ANOVA and two-way ANOVA were used for comparison among multiple groups. Pairwise comparisons between groups were analyzed by the student's *t*-test. *P* values < 0.05 were considered to indicate statistical significance.

3. Results

3.1. EA at ST 36 improved motor function in 5×FAD mice

We assessed motor function and the state of anxiety using the open field test (OFT). No significant differences in the total moving distance or average moving speed were observed in the 3-m mouse group. It is also discovered that age-matched 5×FAD mice tended to show a decrease in the average speed and total distance traveled compared with 6-month-old WT mice. The total distance traveled and the average speed of the 9-m 5×FAD mice decreased significantly in comparison with the age-matched WT ones, however the age-matched EA-ST 36 group mice showed partial restoration of both of these results, but no significant changes were detected in the EA-ST 25 group (Fig. 1B and C). These results indicated that the motor ability of the 5×FAD mice decreased significantly with aging, while EA at ST 36, but not ST 25, improved motor ability. In addition, no statistic difference in time spent in the central region or counts crossing the central area were observed between the groups of different ages, suggesting no anxiety or depression in the mice (Fig. 1D and E). Our results demonstrated that EA at ST 36 significantly improved the deficiency of motor ability in AD mice.

3.2. EA at ST 36 improved the cognitive ability of 5×FAD mice

Next, the novel object recognition test (NORT) was used to assess recognition memory of mice. As illustrated by Fig. 2A, no significant difference in discrimination was detected between the 3-month-old group at 1 and 24 h. The discrimination index of the 6- and 9-m 5×FAD mice decreased in comparison to that of the WT group at 1 h, whereas EA-ST 36 significantly improved the discrimination index (Fig. 2B and C). EA at ST 36 tended to improve the discrimination index of 6- and 9-m 5×FAD mice at 24 h. No changes in the discrimination index were noticed between EA-ST 25 group and 5×FAD mice of all ages at either time. These results showed that EA at ST 36, but not ST 25, significantly improved the cognitive ability of 5×FAD mice.

3.3. EA at ST 36 improved the spatial learning and memory of 5×FAD mice

We did not detect any difference in 5-day escape latency on the Morris Water Maze (MWM) experiment between the groups. The average speed, time spent in the target quadrant, and time crossing the platform on the last day were determined in the 3-month-old mice (Fig. 3A). The 6- and 9-m 5×FAD mice had impaired learning and memory compared with the age-matched WT group, as indicated by the slower escape latency during consecutive trials. Nevertheless, the escape latency was significantly faster in the EA-ST 36 group on training days 4 and 5 compared with that of the 6- and 9-m 5×FAD mice (Fig. 3B and C). Furthermore, the 5×FAD group failed to find the target platform, while the EA-ST 36 group remained in the target quadrant as long as the 6- and 9-m WT mice (Fig. 3D). The time the 5×FAD mice needed to cross the platform on the last day was much less at 6- and 9-months old than the age-matched WT mice; however, EA at ST 36 tended to improve the times (Fig. 3E). We also discovered that the swimming speed of the 9-m

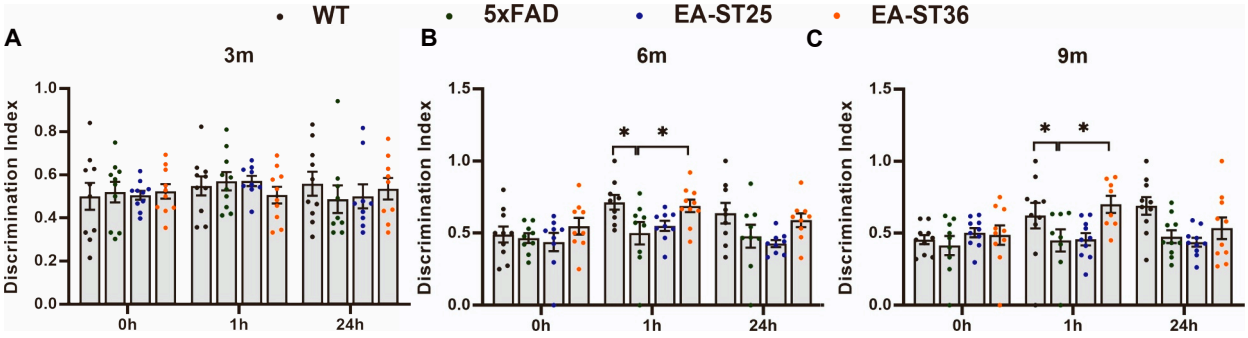

Fig. 2. Effect of EA on the cognitive ability of 5×FAD mice detected by NORT. **(A–C)** The discrimination index of 4 groups (WT, 5×FAD, EA-ST25, EA-ST36) at 3-, 6-, and 9-month-old. (The bars indicate the means ± SEM; n = 10 per group; $*p < 0.05$).

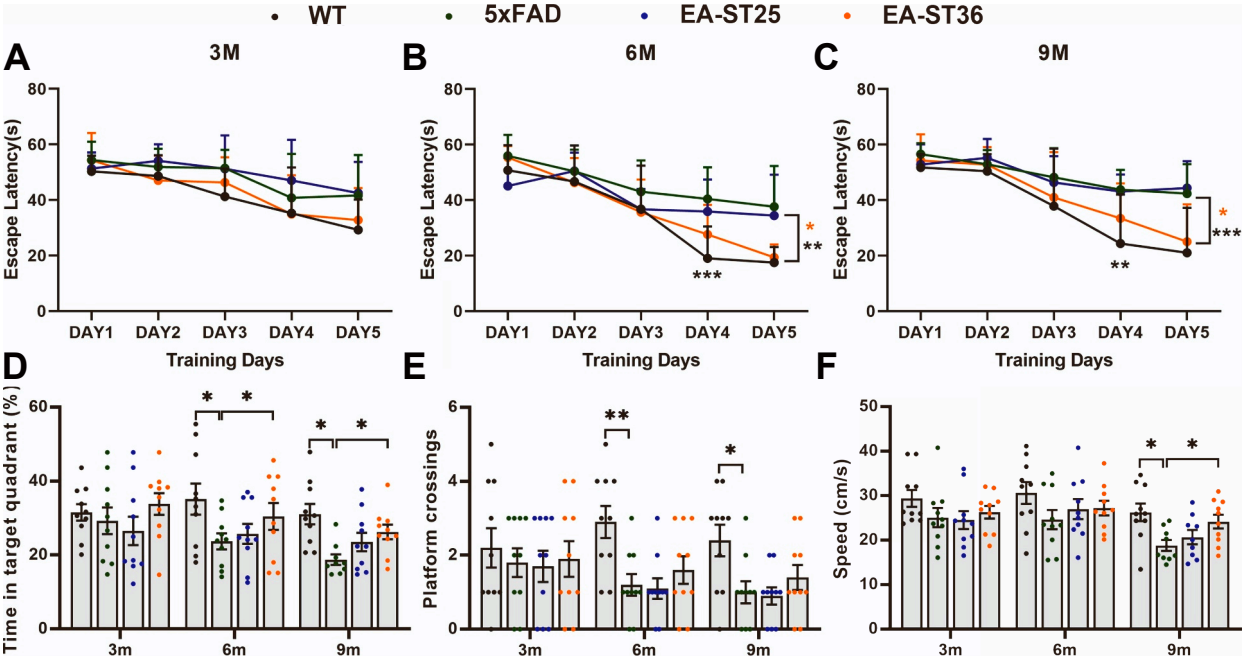

Fig. 3. Effect of EA on the spatial learning and memory of 5×FAD mice detected by MWM. **(A–C)** The latency of 4 groups (WT, 5×FAD, EA-ST25, EA-ST36) in finding a target platform during the 5-day period training trials at 3-, 6-, and 9-month-old. **(D)** Time spent in the target quadrant on the last day without platform. **(E)** Counts crossing the platform area on the last day without platform. **(F)** Swimming speed. (The bars indicate the means ± SEM; n = 10 per group; $*p < 0.05$).

5×FAD mice was less than that of the WT group, while the age-matched EA-ST 36 mice regained their athletic ability (Fig. 3F). However, no significant differences were detected between the EA-ST 25 and 5×FAD groups at any age, suggesting that EA at ST 36, but not ST 25, attenuated the learning as well as motor impairments in the 5×FAD mice.

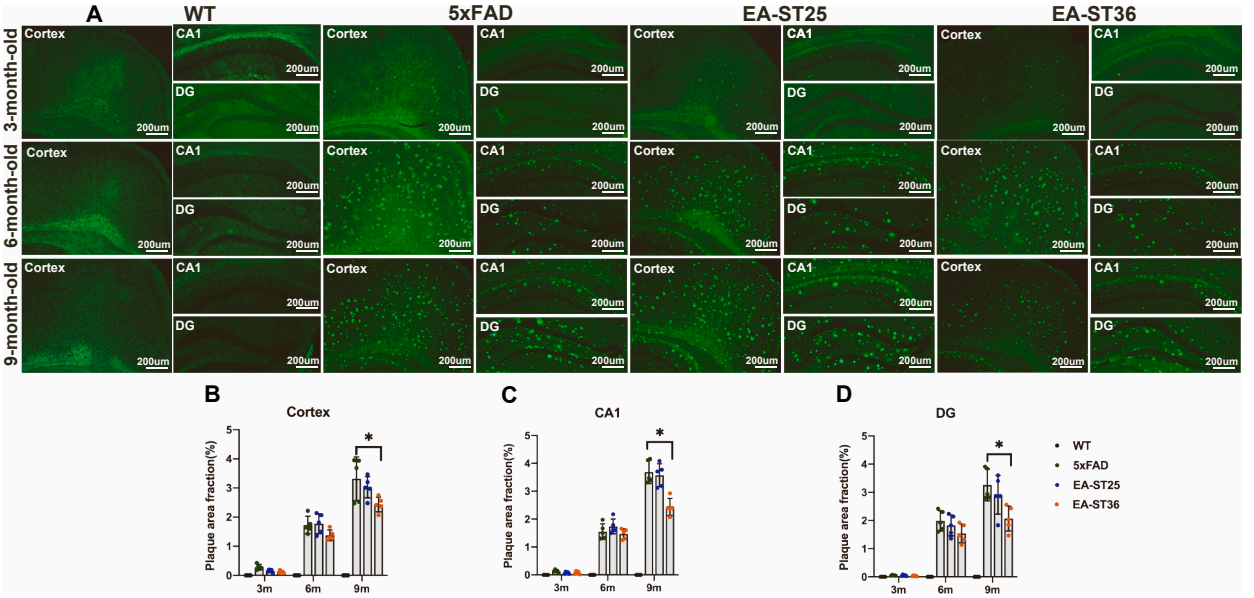

Fig. 4. Effect of EA on Aβ deposition of 5×FAD mice. **(A)** Representative photomicrographs of Thio-S staining in Cortex, CA1 and DG regions of 4 groups (WT, 5×FAD, EA-ST25, EA-ST36) at 3-, 6-, and 9-month-old. **(B, C, D)** Quantification of Thio-S staining levels in Cortex, CA1 and DG regions of different groups. (The bars indicate the means ± SD; n = 5 per group; $*p < 0.05$; Scale bar = 200 μm).

3.4. EA at ST 36 reduced Aβ accumulation in the brain of 5×FAD mice

We compared thioflavin-S-positive plaques between the groups at the cortex, hippocampal CA1, and hippocampal dentate gyrus areas to access the potential impact of EA at ST 36 on Aβ burden. Many studies have shown that WT mice do not produce Aβ deposits in

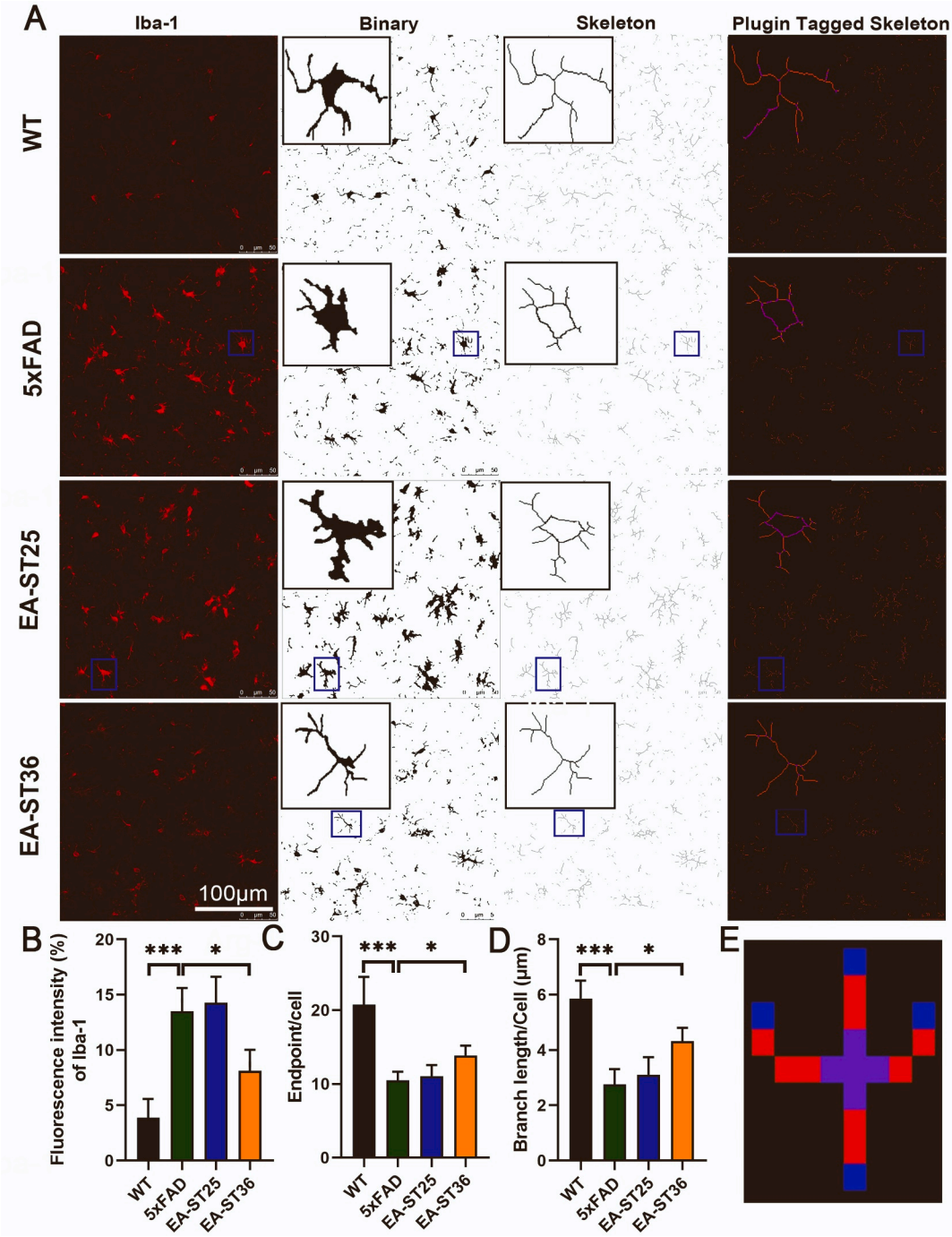

Fig. 5. Effect of EA on microglia activation of 5×FAD mice. **(A)** Representative immunofluorescence photomicrographs of Iba-1 in hippocampus CA1 of 4 groups (WT, 5×FAD, EA-ST25, EA-ST36) at 9-month-old. **(B)** Quantification of Iba-1(+) fluorescence intensity. **(C)** Total endpoint numbers per microglial. **(D)** Total branch length per microglial. **(E)** The skeletonized images are processed using the Analyze Skeleton plugin of Image J software to identify and tag skeletonized processes as orange, endpoints as blue, and junctions as purple. (The bars indicate the means ± SD; n = 5 per group; $*p < 0.05$, $***p < 0.001$; Scale bar = 100 μm)

the brain regardless of age, as shown in Fig. 4A. This analysis demonstrated that the 5×FAD mouse brains exhibited clear age-dependent Aβ deposition (Fig. 4A). However, no statistic difference was detected between 3- and 6-m groups. Notably, a significant decrease in plaque deposits was observed in all three areas of the 9-month-old EA-ST 36 group compared to the age-matched 5×FAD group, while no changes were noted between the EA-ST 25 and 5×FAD groups (Fig. 4B–D). These results suggested that EA at ST 36, but not ST 25, reduced Aβ accumulation in the brain of 5×FAD mice.

3.5. EA at ST 36 reduced the activation of microglia in the brain of 5×FAD mice

Based on previous experiments, we concluded that EA at ST 36 improved motor function and cognitive ability and alleviated Aβ accumulation in 5×FAD mice, particularly in 9-m mice, so we decided to use only 9-month-old mice in our subsequent studies. To investigate the role of EA at ST 36 on the activation of microglia, we stained microglia (Iba-1) in the CA1 hippocampus with red immunofluorescence. The Iba-1 fluorescence intensity was much more pronounced in the 5×FAD and EA-ST 25 groups than in the WT group; however, expression in the EA-ST 36 samples was almost absent with only faint staining (Fig. 5A and B). At the same time, we observed that the microglia in the hippocampus of 5×FAD mice were significantly activated compared with the WT ones, as manifested by larger cell bodies as well as shorter and fewer branches. Referring to the statistical method of a previous study (Fig. 5E) [28], we calculated the total length of the branches and the number of branching endpoints on each cell to mark the activation changes in the microglia. Our results show that the total branch length and endpoints of the microglia decreased in 5×FAD mice in comparison with the WT ones. Nevertheless, these effects could be significantly reversed by EA at ST 36 (Fig. 5C and D). However, no change in activation of the microglia was detected in EA-ST 25 mice compared to the 5×FAD group. Therefore, it was reasonable to speculate that EA at ST 36, but not ST 25, decreased the microglial activation in 5×FAD mice.

3.6. EA at ST 36 suppressed activation of the NLRP3 inflammasome and its production of IL-1β and IL-18 in the brain of 5×FAD mice

As illustrated by Fig. 6A, the expression levels of NLRP3, caspase-1, ASC, IL-1β, and IL-18 in the hippocampus of 5×FAD mice was increased significantly in comparison with those in WT ones, while EA at ST 36 downregulated the levels of all of these proteins (Fig. 6B). Additionally, no significant differences were observed between the EA-ST 25 and 5×FAD groups. Our qRT-PCR results were consistent with our Western blot results, which showed that EA-ST 36 reduced the upregulation of NLRP3, IL-1β, and IL-18 mRNA in 5×FAD mice (Fig. 6C). The results above indicated that EA at ST 36, but not ST 25, inhibited activation of the NLRP3 inflammasome and its production of IL-1β and IL-18 in 5×FAD mice.

4. Discussion

In recent years, a growing number of randomized controlled clinical trials and systematic reviews have shown that EA treatment alone or in combination with other drugs and different acupoints can significantly improve cognitive impairment in AD patients without serious side effects [12,30,31]. In animal experiments, EA significantly improved the spatial learning ability, memory capacity, and emotions (e.g., depression and anxiety) of different AD mouse models in different behavioral experiments, such as the MWM, NORT, and OFT [32,33]. Many clinical trials have been performed using ST 36 as the key acupuncture point for treating or relieving AD [18,34]. Our study found that mice treated with EA at ST 36 had significantly better motor, spatial learning, and memory abilities than did 5×FAD mice.

It is commonly accepted that acupuncture at diverse acupoints has different effects, even on the same disease. The acupoints ST 36, KI 1, GV 20, CV 6, CV 17, SP 10, and LI 20 are the most frequently used in clinical treatment and animal studies of AD [35]. Stimulating these acupoints improves cognitive function in AD by different mechanisms. EA at ST 36 reduces lipopolysaccharide-induced serum levels of all of the cytokines analyzed, including TNF, monocyte chemotactic protein-1, IL-6, and interferon-γ by modulating the vagus nerve [20]. ST 36 has more pronounced anti-inflammatory properties through the vagal–adrenal axis compared to other commonly used acupoints [21,22]. In addition, ST 36 stimulates more brain areas to produce more comprehensive effects [36], such as promoting nerve regeneration [37] and increasing dendritic complexity [38]. Thus, we wondered whether EA at ST 36 could alleviate AD

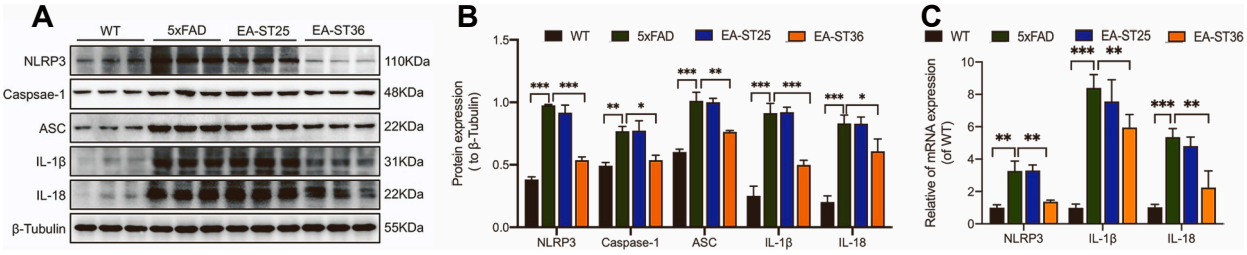

Fig. 6. Effect of EA on the activation of NLRP3 inflammasome and its production IL-1β and IL-18 of 5×FAD mice. **(A, B)** The protein expression of NLRP3, Caspase-1, ASC, IL-1β and IL-18 in the hippocampus of mice were detected by Western Blot. **(C)** The mRNA levels of NLRP3, IL-1β and IL-18 in the hippocampus of all groups were detected by qRT-PCR. (The bars indicate the means ± SD; n = 5 per group; $*p < 0.05$, $**p < 0.01$, $***p < 0.001$).

pathology and cognitive decline by reducing inflammation in the brain.

Many studies of AD have shown that inflammation of the brain, also known as the neuroinflammatory response, is the third most important factor in AD [39,40]. Microglia orchestrate inflammatory reactions in the central nervous system [41]. The accumulation of Aβ has a direct toxic effect on nerve cells and drives the activation of microglia [42]. Early in the disease, Aβ acts on multiple receptors on the surface of microglia, including TLR, CD33, CD36, and TREM2, and microglia transform from a quiescent branching morphology into an activated amoeboid morphology and migrate near plaques to produce pro-inflammatory factors and chemokines and increase the phagocytosis of Aβ, resulting in neuroprotective effects [43,44]. Activated microglia produce a variety of phenotypes. Activated macrophages have been divided into pro-inflammatory (M1) and anti-inflammatory phenotypes (M2). This classification also applies to microglia [45]. Under normal conditions, the low level of inflammation drives microglia to activate towards the anti-inflammatory phenotype, which is involved in tissue repair and phagocytosis [5]. However, in AD, the persistent formation of Aβ drives prolonged activation of microglia, producing inflammatory mediators, including reactive oxygen species, IL-1β, IL-6, IL-8, TNF-α, and chemokines [46]. These inflammatory mediators contribute to convert microglia to the pro-inflammatory phenotype (M1), which not only induces an inflammatory cascade but regulates the expression of the amyloid precursor protein (APP) and protein hydrolysis to promote Aβ deposition [47–49]. The reduced expression of beclin1 in microglia in response to prolonged stimulation by Aβ affects the sorting and phagocytosis of cellular components mediated by receptors, such as TLR, TREM2, CD33, and CD36, and reduces Aβ clearance [50]. Our study shows that EA at ST 36, but not ST 25, significantly reduced Aβ deposition and inhibited the activation of microglia in the hippocampus of 5×FAD mice; thus, ST 36 has potent anti-neuroinflammatory potential.

Clinical studies have reported significant upregulation of NLRP3 inflammasome mRNA and its downstream effector IL-1β in the cerebrospinal fluid of AD patients with varying degrees of disease [51]. NLRP3 is a macromolecular protein consisting of an NLRP3 scaffold and three ASC and caspase-1 precursor components, which regulate the maturation and secretion of inflammatory cytokines, including IL-1β, IL-18, and IL-33 [52,53]. NLRP3 is highly expressed in microglia. Over-activated NLRP3 inflammatory vesicles stimulate the activation of microglia and contribute to their conversion to the pro-inflammatory phenotype (M1) [54]. NLRP3 is a vital event bridging the two core AD pathologies (Aβ and tau) [40]. IL-1β and IL-18 induced by NLRP3 play a unique role in the pathology of AD. Aβ and tau stimulation of NLRP3 inflammatory agents induces the maturation and release of IL-1β. IL-1β upregulates APP and Aβ expression in astrocytes and promotes tau phosphorylation through the MAPK-p38 pathway to form NFTs [55]. IL-18 upregulates γ-secretase and promotes Aβ production while promoting tau hyperphosphorylation via glycogen synthase kinase-3 beta [56]. Growing evidence indicates that activation of NLRP3 is a driver of AD pathology [40]. The ASC, a component of NLRP3, forms a complex with Aβ that inhibits microglia phagocytosis and amplifies the NLRP3 inflammatory response while inducing cellular scorching via gasdermin-D [57]. Drugs targeting the NLRP3 inflammasome have emerged as a new strategy for treating AD because inhibiting the NLRP3 inflammasome reduces inflammation while preserving microglial function [58]. Unfortunately, no drug directly inhibits NLRP3. Only NSAIDs, which target volume-regulated anion channels, have shown good results [59]. Moreover, EA inhibits activation of the NLRP3 inflammasome through several different pathways, including the microRNA, NF-κB/NLRP3, ATP/P2X7R/NLRP3, and ROS/TXNIP/NLRP3 signaling pathways, which are related to reducing the inflammatory response [60]. In our study, EA at ST 36 significantly inhibited activation of the NLRP3 inflammasome signaling pathway in the hippocampus of 5×FAD mice, which may be directly related to its ability to reduce the proliferation and activation of microglia. Moreover, peripheral inflammatory cytokines play a key role in triggering the activation of microglia in AD [61]. Therefore, EA at ST 36 may inhibit the levels of peripheral inflammatory cytokines to affect the activation of microglia or the NLRP3 inflammasome in AD. However, more evidence is needed to prove this hypothesis.

As a consequence, this study shows that EA at ST 36, but not ST 25, attenuated Aβ deposition, alleviated activation of microglia by reducing activation of the NLRP3 inflammasome in the hippocampus, and improved motor and cognitive deficits in 5×FAD mice. Our study shows that ST 36 may be a specific acupoint to improve the condition of AD patients.

Author contribution statement

Jie Wang, Hong Ni: Conceived and designed the experiments; Performed the experiments; Wrote the paper.
Dezhi Liu: Conceived and designed the experiments; Contributed reagents, materials, analysis tools or data; Wrote the paper.
Qimeng Wang: Performed the experiments.
Jiaoqi Ren: Analyzed and interpreted the data; Wrote the paper.
Xing Li, Yue Wu: Analyzed and interpreted the data.

Funding statement

Dezhi Liu was supported by Grants from the Traditional Chinese Medicine Research Program of Shanghai Municipal Health Commission [2020LZ002]; Shanghai Health Committee [201840154]; Science and Technology Innovation Plan of Shanghai Science and Technology Commission [22S31902300].

Dr Jie Wang was supported by Siming Youth Foundation of Shuguang Hospital [SGKJ-202101].

Data availability statement

Data will be made available on request.

Declaration of competing interest

The authors declare that they have no known competing financial interests or personal relationships that could have appeared to influence the work reported in this paper.

Appendix A. Supplementary data

Supplementary data related to this article can be found at https://doi.org/10.1016/j.heliyon.2023.e16755.

References

[1] J.M. Long, D.M. Holtzman, Alzheimer disease: an update on pathobiology and treatment strategies, Cell 179 (2) (2019) 312–339.
[2] H.W. Querfurth, F.M. LaFerla, Alzheimer's disease, N. Engl. J. Med. 362 (4) (2010) 329–344.
[3] V. Calsolaro, P. Edison, Neuroinflammation in Alzheimer's disease: current evidence and future directions, Alzheimers Dement. 12 (6) (2016) 719–732.
[4] Y. Peng, J. Wang, C. Zheng, Study on dynamic characteristics' change of hippocampal neuron reduced models caused by the Alzheimer's disease, J. Biol. Dynam. 10 (2016) 250–262.
[5] M.T. Heneka, M.J. Carson, J. El Khoury, G.E. Landreth, F. Brosseron, D.L. Feinstein, A.H. Jacobs, T. Wyss-Coray, J. Vitorica, R.M. Ransohoff, K. Herrup, S. A. Frautschy, B. Finsen, G.C. Brown, A. Verkhratsky, K. Yamanaka, J. Koistinaho, E. Latz, A. Halle, G.C. Petzold, T. Town, D. Morgan, M.L. Shinohara, V. H. Perry, C. Holmes, N.G. Bazan, D.J. Brooks, S. Hunot, B. Joseph, N. Deigendesch, O. Garaschuk, E. Boddeke, C.A. Dinarello, J.C. Breitner, G.M. Cole, D. T. Golenbock, M.P. Kummer, Neuroinflammation in Alzheimer's disease, Lancet Neurol. 14 (4) (2015) 388–405.
[6] S.M. Allan, N.J. Rothwell, Inflammation in central nervous system injury, Philos. Trans. R. Soc. Lond. B Biol. Sci. 358 (1438) (2003) 1669–1677.
[7] M.T. Heneka, M.K. O'Banion, Inflammatory processes in Alzheimer's disease, J. Neuroimmunol. 184 (1-2) (2007) 69–91.
[8] D. Krstic, A. Madhusudan, J. Doehner, P. Vogel, T. Notter, C. Imhof, A. Manalastas, M. Hilfiker, S. Pfister, C. Schwerdel, C. Riether, U. Meyer, I. Knuesel, Systemic immune challenges trigger and drive Alzheimer-like neuropathology in mice, J. Neuroinflammation 9 (2012) 151.
[9] M. Pennisi, R. Crupi, R. Di Paola, M.L. Ontario, R. Bella, E.J. Calabrese, R. Crea, S. Cuzzocrea, V. Calabrese, Inflammasomes, hormesis, and antioxidants in neuroinflammation: role of NRLP3 in Alzheimer disease, J. Neurosci. Res. 95 (7) (2017) 1360–1372.
[10] K. Zhou, L. Shi, Y. Wang, S. Chen, J. Zhang, Recent advances of the NLRP3 inflammasome in central nervous system disorders, J. Immunol. Res. 2016 (2016), 9238290.
[11] R. Lin, J. Chen, X. Li, J. Mao, Y. Wu, P. Zhuo, Y. Zhang, W. Liu, J. Huang, J. Tao, L.D. Chen, Electroacupuncture at the Baihui acupoint alleviates cognitive impairment and exerts neuroprotective effects by modulating the expression and processing of brain-derived neurotrophic factor in APP/PS1 transgenic mice, Mol. Med. Rep. 13 (2) (2016) 1611–1617.
[12] J. Zhou, W. Peng, M. Xu, W. Li, Z. Liu, The effectiveness and safety of acupuncture for patients with Alzheimer disease: a systematic review and meta-analysis of randomized controlled trials, Medicine (Baltim.) 94 (22) (2015) e933.
[13] H.J. Kim, B.S. Jeon, Is acupuncture efficacious therapy in Parkinson's disease? J. Neurol. Sci. 341 (1-2) (2014) 1–7.
[14] X.T. Su, N. Sun, N. Zhang, L.Q. Wang, X. Zou, J.L. Li, J.W. Yang, G.X. Shi, C.Z. Liu, Effectiveness and safety of acupuncture for vascular cognitive impairment: a systematic review and meta-analysis, Front. Aging Neurosci. 13 (2021), 692508.
[15] J. Jiang, K. Gao, Y. Zhou, A. Xu, S. Shi, G. Liu, Z. Li, Electroacupuncture treatment improves learning-memory ability and brain glucose metabolism in a mouse model of alzheimer's disease: using Morris water maze and micro-PET, Evid. Based Complement Alternat. Med. 2015 (2015), 142129.
[16] J. Jiang, N. Ding, K. Wang, Z. Li, Electroacupuncture could influence the expression of IL-1beta and NLRP3 inflammasome in Hippocampus of alzheimer's disease animal model, Evid. Based Complement Alternat. Med. 2018 (2018), 8296824.
[17] X. Zheng, W. Lin, Y. Jiang, K. Lu, W. Wei, Q. Huo, S. Cui, X. Yang, M. Li, N. Xu, C. Tang, J.X. Song, Electroacupuncture ameliorates beta-amyloid pathology and cognitive impairment in Alzheimer disease via a novel mechanism involving activation of TFEB (transcription factor EB), Autophagy 17 (11) (2021) 3833–3847.
[18] Y. Zhou, J. Jin, Effect of acupuncture given at the HT 7, ST 36, ST 40 and KI 3 acupoints on various parts of the brains of Alzheimer' s disease patients, Acupunct. Electro-Ther. Res. 33 (1-2) (2008) 9–17.
[19] L. Ulloa, S. Quiroz-Gonzalez, R. Torres-Rosas, Nerve stimulation: immunomodulation and control of inflammation, Trends Mol. Med. 23 (12) (2017) 1103–1120.
[20] R. Torres-Rosas, G. Yehia, G. Pena, P. Mishra, M. del Rocio Thompson-Bonilla, M.A. Moreno-Eutimio, L.A. Arriaga-Pizano, A. Isibasi, L. Ulloa, Dopamine mediates vagal modulation of the immune system by electroacupuncture, Nat. Med. 20 (3) (2014) 291–295.
[21] S. Liu, Z.F. Wang, Y.S. Su, R.S. Ray, X.H. Jing, Y.Q. Wang, Q. Ma, Somatotopic organization and intensity dependence in driving distinct NPY-expressing sympathetic pathways by electroacupuncture, Neuron 108 (3) (2020) 436–450 e437.
[22] S. Liu, Z. Wang, Y. Su, L. Qi, W. Yang, M. Fu, X. Jing, Y. Wang, Q. Ma, A neuroanatomical basis for electroacupuncture to drive the vagal-adrenal axis, Nature 598 (7882) (2021) 641–645.
[23] J.G. Song, H.H. Li, Y.F. Cao, X. Lv, P. Zhang, Y.S. Li, Y.J. Zheng, Q. Li, P.H. Yin, S.L. Song, H.Y. Wang, X.R. Wang, Electroacupuncture improves survival in rats with lethal endotoxemia via the autonomic nervous system, Anesthesiology 116 (2) (2012) 406–414.
[24] V. Landel, K. Baranger, I. Virard, B. Loriod, M. Khrestchatisky, S. Rivera, P. Benech, F. Feron, Temporal gene profiling of the 5XFAD transgenic mouse model highlights the importance of microglial activation in Alzheimer's disease, Mol. Neurodegener. 9 (2014) 33.
[25] C.V. Vorhees, M.T. Williams, Morris water maze: procedures for assessing spatial and related forms of learning and memory, Nat. Protoc. 1 (2) (2006) 848–858.
[26] E. Dere, J.P. Huston, M.A. De Souza Silva, The pharmacology, neuroanatomy and neurogenetics of one-trial object recognition in rodents, Neurosci. Biobehav. Rev. 31 (5) (2007) 673–704.
[27] S. Oddo, A. Caccamo, I.F. Smith, K.N. Green, F.M. LaFerla, A dynamic relationship between intracellular and extracellular pools of Abeta, Am. J. Pathol. 168 (1) (2006) 184–194.
[28] H. Morrison, K. Young, M. Qureshi, R.K. Rowe, J. Lifshitz, Quantitative microglia analyses reveal diverse morphologic responses in the rat cortex after diffuse brain injury, Sci. Rep. 7 (1) (2017), 13211.
[29] S.M. Ayuk, H. Abrahamse, N.N. Houreld, The role of photobiomodulation on gene expression of cell adhesion molecules in diabetic wounded fibroblasts in vitro, J. Photochem. Photobiol., B 161 (2016) 368–374.
[30] L. Zhao, J. Chen, Y. Li, X. Sun, X. Chang, H. Zheng, B. Gong, Y. Huang, M. Yang, X. Wu, X. Li, F. Liang, The long-term effect of acupuncture for migraine prophylaxis: a randomized clinical trial, JAMA Intern. Med. 177 (4) (2017) 508–515.
[31] W. Peng, J. Zhou, M. Xu, Q. Feng, L. Bin, Z. Liu, The effect of electroacupuncture combined with donepezil on cognitive function in Alzheimer's disease patients: study protocol for a randomized controlled trial, Trials 18 (1) (2017) 301.
[32] B. Yang, M. He, X. Chen, M. Sun, T. Pan, X. Xu, X. Zhang, Q. Gong, Y. Zhao, Z. Jin, Z. Cheng, Acupuncture effect assessment in APP/PS1 transgenic mice: on regulating learning-memory abilities, gut microbiota, and microbial metabolites, Comput. Math. Methods Med. 2022 (2022), 1527159.
[33] J. Jiang, H. Liu, Z. Wang, H. Tian, S. Wang, J. Yang, J. Ren, Electroacupuncture could balance the gut microbiota and improve the learning and memory abilities of Alzheimer's disease animal model, PLoS One 16 (11) (2021), e0259530.

[34] W. Gu, X.X. Jin, Y.J. Zhang, Z.J. Li, Y. Kong, [Clinical observation of Alzheimer's disease treated with acupuncture], Zhongguo Zhen Jiu. 34 (12) (2014) 1156–1160.
[35] C.C. Yu, C.Y. Ma, H. Wang, L.H. Kong, Y. Zhao, F. Shen, M. Wu, Effects of acupuncture on alzheimer's disease: evidence from neuroimaging studies, Chin. J. Integr. Med. 25 (8) (2019) 631–640.
[36] Y.J. Lu, X.W. Cai, G.F. Zhang, Y. Huang, C.Z. Tang, B.C. Shan, S.Y. Cui, J.Q. Chen, S.S. Qu, Z. Zhong, X.S. Lai, G.Z. Steiner, Long-term acupuncture treatment has a multi-targeting regulation on multiple brain regions in rats with Alzheimer's disease: a positron emission tomography study, Neural. Regen. Res. 12 (7) (2017) 1159–1165.
[37] M.H. Nam, K.S. Ahn, S.H. Choi, Acupuncture stimulation induces neurogenesis in adult brain, Int. Rev. Neurobiol. 111 (2013) 67–90.
[38] B.H. Kan, J.C. Yu, L. Zhao, J. Zhao, Z. Li, Y.R. Suo, J.X. Han, Acupuncture improves dendritic structure and spatial learning and memory ability of Alzheimer's disease mice, Neural. Regen. Res. 13 (8) (2018) 1390–1395.
[39] F. Leng, P. Edison, Neuroinflammation and microglial activation in Alzheimer disease: where do we go from here? Nat. Rev. Neurol. 17 (3) (2021) 157–172.
[40] C. Ising, C. Venegas, S. Zhang, H. Scheiblich, S.V. Schmidt, A. Vieira-Saecker, S. Schwartz, S. Albasset, R.M. McManus, D. Tejera, A. Griep, F. Santarelli, F. Brosseron, S. Opitz, J. Stunden, M. Merten, R. Kayed, D.T. Golenbock, D. Blum, E. Latz, L. Buee, M.T. Heneka, NLRP3 inflammasome activation drives tau pathology, Nature 575 (7784) (2019) 669–673.
[41] H. Sarlus, M.T. Heneka, Microglia in Alzheimer's disease, J. Clin. Invest. 127 (9) (2017) 3240–3249.
[42] S.H. Baik, S. Kang, S.M. Son, I. Mook-Jung, Microglia contributes to plaque growth by cell death due to uptake of amyloid beta in the brain of Alzheimer's disease mouse model, Glia 64 (12) (2016) 2274–2290.
[43] L. Zhong, Y. Xu, R. Zhuo, T. Wang, K. Wang, R. Huang, D. Wang, Y. Gao, Y. Zhu, X. Sheng, K. Chen, N. Wang, L. Zhu, D. Can, Y. Marten, M. Shinohara, C.C. Liu, D. Du, H. Sun, L. Wen, H. Xu, G. Bu, X.F. Chen, Soluble TREM2 ameliorates pathological phenotypes by modulating microglial functions in an Alzheimer's disease model, Nat. Commun. 10 (1) (2019) 1365.
[44] L. Zhong, Z. Wang, D. Wang, Z. Wang, Y.A. Martens, L. Wu, Y. Xu, K. Wang, J. Li, R. Huang, D. Can, H. Xu, G. Bu, X.F. Chen, Amyloid-beta modulates microglial responses by binding to the triggering receptor expressed on myeloid cells 2 (TREM2), Mol. Neurodegener. 13 (1) (2018) 15.
[45] B. Zhang, C. Gaiteri, L.G. Bodea, Z. Wang, J. McElwee, A.A. Podtelezhnikov, C. Zhang, T. Xie, L. Tran, R. Dobrin, E. Fluder, B. Clurman, S. Melquist, M. Narayanan, C. Suver, H. Shah, M. Mahajan, T. Gillis, J. Mysore, M.E. MacDonald, J.R. Lamb, D.A. Bennett, C. Molony, D.J. Stone, V. Gudnason, A.J. Myers, E. E. Schadt, H. Neumann, J. Zhu, V. Emilsson, Integrated systems approach identifies genetic nodes and networks in late-onset Alzheimer's disease, Cell 153 (3) (2013) 707–720.
[46] T. Wyss-Coray, J. Rogers, Inflammation in Alzheimer disease-a brief review of the basic science and clinical literature, Cold Spring Harb. Perspect. Med. 2 (1) (2012) a006346.
[47] G. Thiabaud, S. Pizzocaro, R. Garcia-Serres, J.M. Latour, E. Monzani, L. Casella, Heme binding induces dimerization and nitration of truncated beta-amyloid peptide Abeta16 under oxidative stress, Angew Chem. Int. Ed. Engl. 52 (31) (2013) 8041–8044.
[48] M.T. Heneka, M.P. Kummer, A. Stutz, A. Delekate, S. Schwartz, A. Vieira-Saecker, A. Griep, D. Axt, A. Remus, T.C. Tzeng, E. Gelpi, A. Halle, M. Korte, E. Latz, D. T. Golenbock, NLRP3 is activated in Alzheimer's disease and contributes to pathology in APP/PS1 mice, Nature 493 (7434) (2013) 674–678.
[49] S.H. Cho, B. Sun, Y. Zhou, T.M. Kauppinen, B. Halabisky, P. Wes, R.M. Ransohoff, L. Gan, CX3CR1 protein signaling modulates microglial activation and protects against plaque-independent cognitive deficits in a mouse model of Alzheimer disease, J. Biol. Chem. 286 (37) (2011) 32713–32722.
[50] K.M. Lucin, C.E. O'Brien, G. Bieri, E. Czirr, K.I. Mosher, R.J. Abbey, D.F. Mastroeni, J. Rogers, B. Spencer, E. Masliah, T. Wyss-Coray, Microglial beclin 1 regulates retromer trafficking and phagocytosis and is impaired in Alzheimer's disease, Neuron 79 (5) (2013) 873–886.
[51] M. Saresella, F. La Rosa, F. Piancone, M. Zoppis, I. Marventano, E. Calabrese, V. Rainone, R. Nemni, R. Mancuso, M. Clerici, The NLRP3 and NLRP1 inflammasomes are activated in Alzheimer's disease, Mol. Neurodegener. 11 (2016) 23.
[52] A. Abderrazak, T. Syrovets, D. Couchie, K. El Hadri, B. Friguet, T. Simmet, M. Rouis, NLRP3 inflammasome: from a danger signal sensor to a regulatory node of oxidative stress and inflammatory diseases, Redox Biol. 4 (2015) 296–307.
[53] D. De Nardo, E. Latz, NLRP3 inflammasomes link inflammation and metabolic disease, Trends Immunol. 32 (8) (2011) 373–379.
[54] A.G. Wu, X.G. Zhou, G. Qiao, L. Yu, Y. Tang, L. Yan, W.Q. Qiu, R. Pan, C.L. Yu, B.Y. Law, D.L. Qin, J.M. Wu, Targeting microglial autophagic degradation in NLRP3 inflammasome-mediated neurodegenerative diseases, Ageing Res. Rev. 65 (2021), 101202.
[55] W.S. Griffin, L. Liu, Y. Li, R.E. Mrak, S.W. Barger, Interleukin-1 mediates Alzheimer and Lewy body pathologies, J. Neuroinflammation 3 (2006) 5.
[56] J.O. Ojala, E.M. Sutinen, A. Salminen, T. Pirttila, Interleukin-18 increases expression of kinases involved in tau phosphorylation in SH-SY5Y neuroblastoma cells, J. Neuroimmunol. 205 (1-2) (2008) 86–93.
[57] L.L. Friker, H. Scheiblich, I.V. Hochheiser, R. Brinkschulte, D. Riedel, E. Latz, M. Geyer, M.T. Heneka, Beta-amyloid clustering around ASC fibrils boosts its toxicity in microglia, Cell Rep. 30 (11) (2020) 3743–3754 e3746.
[58] C.S. White, C.B. Lawrence, D. Brough, J. Rivers-Auty, Inflammasomes as therapeutic targets for Alzheimer's disease, Brain Pathol. 27 (2) (2017) 223–234.
[59] M.J. Daniels, J. Rivers-Auty, T. Schilling, N.G. Spencer, W. Watremez, V. Fasolino, S.J. Booth, C.S. White, A.G. Baldwin, S. Freeman, R. Wong, C. Latta, S. Yu, J. Jackson, N. Fischer, V. Koziel, T. Pillot, J. Bagnall, S.M. Allan, P. Paszek, J. Galea, M.K. Harte, C. Eder, C.B. Lawrence, D. Brough, Fenamate NSAIDs inhibit the NLRP3 inflammasome and protect against Alzheimer's disease in rodent models, Nat. Commun. 7 (2016), 12504.
[60] M. Yuan, D. Wang, J. Yang, H. Lan, The NLR family pyrin domain containing 3 inflammasome in the mechanism of electroacupuncture: current status and future perspectives, Front. Aging Neurosci. 14 (2022), 913881.
[61] D.A. Dionisio-Santos, J.A. Olschowka, M.K. O'Banion, Exploiting microglial and peripheral immune cell crosstalk to treat Alzheimer's disease, J. Neuroinflammation 16 (1) (2019) 74.